catalysts

MDPI

Advanced Oxidation Process for Degradation of Carbamazepine from Aqueous Solution: Influence of Metal Modified Microporous, Mesoporous Catalysts on the Ozonation Process

Soudabeh Saeid [1], Matilda Kråkström [2], Pasi Tolvanen [1], Narendra Kumar [1,*], Kari Eränen [1], Jyri-Pekka Mikkola [1,3], Leif Kronberg [2], Patrik Eklund [2], Markus Peurla [4], Atte Aho [1], Andrey Shchukarev [3] and **Tapio Salmi [1,*]**

[1] Laboratory of Industrial Chemistry and Reaction Engineering, Johan Gadolin Process Chemistry Centre, Åbo Akademi University, Biskopsgatan 8, FI-20500 Åbo/Turku, Finland; soudabeh.saeid@abo.fi (S.S.); pasi.tolvanen@abo.fi (P.T.); kari.eranen@abo.fi (K.E.); jyri-pekka.mikkola@abo.fi (J.-P.M.); atte.aho@abo.fi (A.A.)

[2] Laboratory of Organic Chemistry, Johan Gadolin Process Chemistry Centre, Åbo Akademi University, Biskopsgatan 8, FI-20500 Åbo/Turku, Finland; matilda.krakstrom@abo.fi (M.K.); leif.kronberg@abo.fi (L.K.); patrik.j.eklund@abo.fi (P.E.)

[3] Technical Chemistry Department of Chemistry Chemical-Biological Center, Umeå University, SE-90187 Umeå, Sweden; andrey.shchukarev@umu.se

[4] Institue of Biomedicin, University of Turku, Kiinamyllynkatu 10, FI-205210 Turku, Finland; markus.peurla@utu.fi

* Correspondence: narendra.kumar@abo.fi (N.K.); tapio.salmi@abo.fi (T.S.)

check for updates

Abstract: Carbamazepine (CBZ), a widely used pharmaceutical compound, is one of the most detected drugs in surface waters. The purpose of this work was to identify an active and durable catalyst, which, in combination with an ozonation process, could be used to remove CBZ and its degradation products. It was found that the CBZ was completely transformed after ozonation within the first minutes of the treatment. However, the resulting degradation products, 1-(2-benzaldehyde)-4-hydro-(1H,3H)-quinazoline-2-one (BQM) and 1-(2-benzaldehyde)-(1H,3H)-quinazoline-2,4-dione (BQD), were more resistant during the ozonation process. The formation and degradation of these products were studied in more detail and a thorough catalytic screening was conducted to reveal the reaction kinetics of both the CBZ and its degradation products. The work was performed by non-catalytic ozonation and with six different heterogeneous catalysts (Pt-MCM-41-IS, Ru-MCM-41-IS, Pd-H-Y-12-EIM, Pt-H-Y-12-EIM, Pd-H-Beta-300-EIM and Cu-MCM-41-A-EIM) operating at two temperatures 20 °C and 50 °C. The influence of temperature on degradation kinetics of CBZ, BQM and BQD was studied. The results exhibited a notable difference in the catalytic behavior by varying temperature. The higher reactor temperature (50 °C) showed a higher activity of the catalysts but a lower concentration of dissolved ozone. Most of the catalysts exhibited higher removal rate for BQM and BQD compared to non-catalytic experiments in both temperatures. The Pd-H-Y-12-EIM catalyst illustrated a higher degradation rate of by-products at 50 °C compared to other catalysts.

Keywords: carbamazepine; ozone; zeolites; catalysts synthesis and characterization; catalytic ozonation

1. Introduction

The frequent appearance of pharmaceuticals as high as mg/L levels in the in ground water and surface waters has been reported in several studies during the last decades [1]. A notable attention has been attracted due to their potential hazard effects on the aquatic ecosystem and human health [2,3]. An emerging concern exists of what exactly happens with the pharmaceutical contaminants in the aquatic environment. The origin of these compounds comes from the fact that they have been employed in several domains of the human activity, for example, human medication, veterinary purposes and aquaculture, as well as large concentrations of them leaking into the sea from pharmaceutical industries. Conventional wastewater treatment is not able to efficiently eliminate most of these pharmaceuticals from wastewaters, not to mention their degradation products [4,5].

Carbamazepine (5H-dibenzo (b,f) azepine-5-carboxamide, shortly CBZ) is a psychiatric pharmaceutical used for treatment of epilepsy and trigeminal neuralgia a chronic pain disorder [6]. CBZ was displayed in a list of essential medicine requirements for a basic health-care in the World Health Organization (WHO) Model List of Essential Medicines (March 2017) in the group of anticonvulsant and antiepileptic pharmaceuticals [7]. Only 28% of CBZ is metabolized by the human body, while the rest is excreted during urination. Before that, it is enzymatically transformed to 10, 11-epoxy-10, 11-dihydro-CBM, and from the hydrolysis of these intermediates, CBZ-diOH is produced. For this reason, CBZ-diOH was one the most abundant CBZ compounds detected in water [8]. CBZ is one of the commonly detected compounds in the effluents. It is resistant against biodegradation, and sometimes the concentration in the effluent has been larger than influent, perhaps due to the conjugates originating from the parent compounds, i.e., hydrolysis through biological treatment [9]. The CBZ and metabolite removal efficiency was −11–18% toward human waste treatment plants, −40% to 25% in the sewage treatment plants and −100–56% in hospital wastewater treatment plants. The concentration of CBZ in the influent and effluent samples were abnormal, this is due to the fact of the low removal rate of CBZ [8].

CBZ has been detected as good as everywhere in the Baltic Sea, in Northern Europe. However, owing to the long turnover time (a very long half-life time in the Baltic Sea, exceeding 3.5 years) and a low elimination rate of CBZ, the wastewater treatment plants exhibit negative removal efficiencies (for instance in Finland with a −41% removal efficiency in wastewater treatment plants). Consequently, it is estimated that more than 55 tons of CBZ has accumulated in the Baltic Sea [10]. CBZ has been detected in the surface water of Milan up to 100 ng/L concentration and it is most frequent drug found in Serbian rivers [11,12]. The research of German and Portuguese surface waters revealed that CBZ and its metabolites were detected to 5000 ng/L in the surface waters, which they were barely decomposed during the wastewater treatment [13].

Significant concentrations of CBZ and five of its metabolites have been detected in urban groundwater in the Spanish rivers Poble Sec and Besòs. Moreover, at the delta of Besòs restored via a river polluted through treated effluent from several treatment plants, CBZ and two of CBZ hydroxyl metabolites were not eliminated following those degrading conditions [14]. Moreover, CBZ was detected in Germany, in the form of the human metabolites, and transformation by-products of CBZ in the several groundwater springs, surface waters and treated wastewater. The genotoxicity of these compounds determined by the so-called silico method (distributed structure-searchable toxicity). These research results revealed that these contaminants have a potential hazard to mammalians, including human beings [15].

The presence of CBZ in the environment poses a potential risk to the aquatic life and human health. This has led to increasing attention to the elimination of CBZ compound through the wastewater treatment plants before discharge into the water basin [16–18]. Several methods have been proposed for the removal of CBZ from wastewaters, for instance, an adsorptive method utilizing biosynthesized hematite nanoparticles. This study did not eliminate the pollutants but instead they were accumulated and pollutants were transferred from aqueous solution to the adsorbent phase [19]. Some another studies concerning an activated sludge system consisting of a membrane bioreactor, the removal was

rather low, around 35% due to of recalcitrance [20], or gamma irradiation coupled with microbiological treatment. With this technology, almost 99% of CBZ could be removed, as well as decreasing the TOC by 80%. However the treatment duration was 250 h, which is a quite long period [21]. Advanced oxidation processes (AOP) have as well been applied for degradation of CBZ such as, radiation-induced activation of peroxymonosulfate, which was reported by Wang et al. [16]. In this investigation, nine intermediate products were detected, and the scientists observed that the limiting step for CBZ mineralization in the system was the decomposition of CBZ intermediates. Low mineralization and hazard intermediates were the biggest obstacles with most of the CBZ treatment trials in the study.

Ozonation has been proposed and applied as a method for removing pharmaceuticals from hospital wastewaters, both in a laboratory and pilot scale. In the laboratory scale, the removal has been successful [22]. Besides, ozonation as an additional treatment step in wastewater treatment has become generally acknowledge for eliminating pharmaceuticals and other micro-pollutants [23]. To improve the ozonation process, more research is needed to study the formation of hydroxyl radicals and the formation of dangerous degradation products of ozonation [9]. Ozonation of CBZ gives some resistant by-products due to the ozone reaction by the olefin group in CBZ, producing an ozonide, which divides the double bond [24]. The major identified by-products from ozonation of CBZ were BQM and BQD [25]. Some methods have been proposed to improve the ozonation of CBZ due to reducing the by-product such as combination by soil aquifer treatment column that enhances degradation of BQD yet the other by-products were more resistance up to 5–6 days [26].

Catalytic ozonation is recommended as an AOP for wastewater treatment, due to enhancing the removal efficiency and its potential to mineralize the organic compounds created. Catalysts improve the decomposition of ozone in the water to produce extremely active hydroxyl radicals [27,28]. Several studies have revealed that coupling ozonation to heterogeneous catalysis is very efficient in oxidizing pharmaceuticals from wastewater. For instance, ozonation combined with a granular activated carbon (GAC) filter can dramatically diminish the CBZ content and its human metabolites [15,29]. Zeolite catalysts exhibited an improvement in the ozonation of the pharmaceutical compound paracetamol [30] and ibuprofen [31]. Moreover, loading of the metals on zeolite catalysts increases the catalytic ozonation efficiency [32].

In the current work, non-catalytic and catalytic ozonation was employed to study the removal of CBZ and its by-products in aqueous solutions. The task is challenging because the degradation rates of the by-products are relatively low. A high concentration of CBZ (30 mg/L) was selected to study the kinetics of the by-products of the degradation. For this purpose, the main products were isolated, and their concentration was monitored with high performance liquid chromatography (HPLC). In order to optimize the degradation of the by-products, the catalysts Pt-MCM-41-IS, Ru-MCM-41-IS, Pd-H-Y-12-EIM, Pt-H-Y-12-EIM, Pd-H-Beta-300-EIM and Cu-MCM-41-A-EIM were used, at two different reaction temperatures. The catalysts were characterized with revealed methods to explain their activities in the experiments.

2. Results and Discussion

2.1. Physico-Chemical Characterization Results: Catalyst Structure and Surface Properties

2.1.1. Transmission Electron Microscopy

The TEM images of (a) Pt-MCM-41-IS, (b) Ru-MCM-41-IS, (c) Pd-H-Y-12-EIM, (d) Pt-H-Y-12-EIM, (e) Pd-H-Beta-300-EIM and (f) Cu-MCM-41-A-EIM catalysts and Pt, Ru, Pd and Cu particle size distributions presented in the form of histograms, are given in Figure 1a–f. The average metal particle size and the distributions were measured and counted from the TEM images, which are displayed in Table 1.
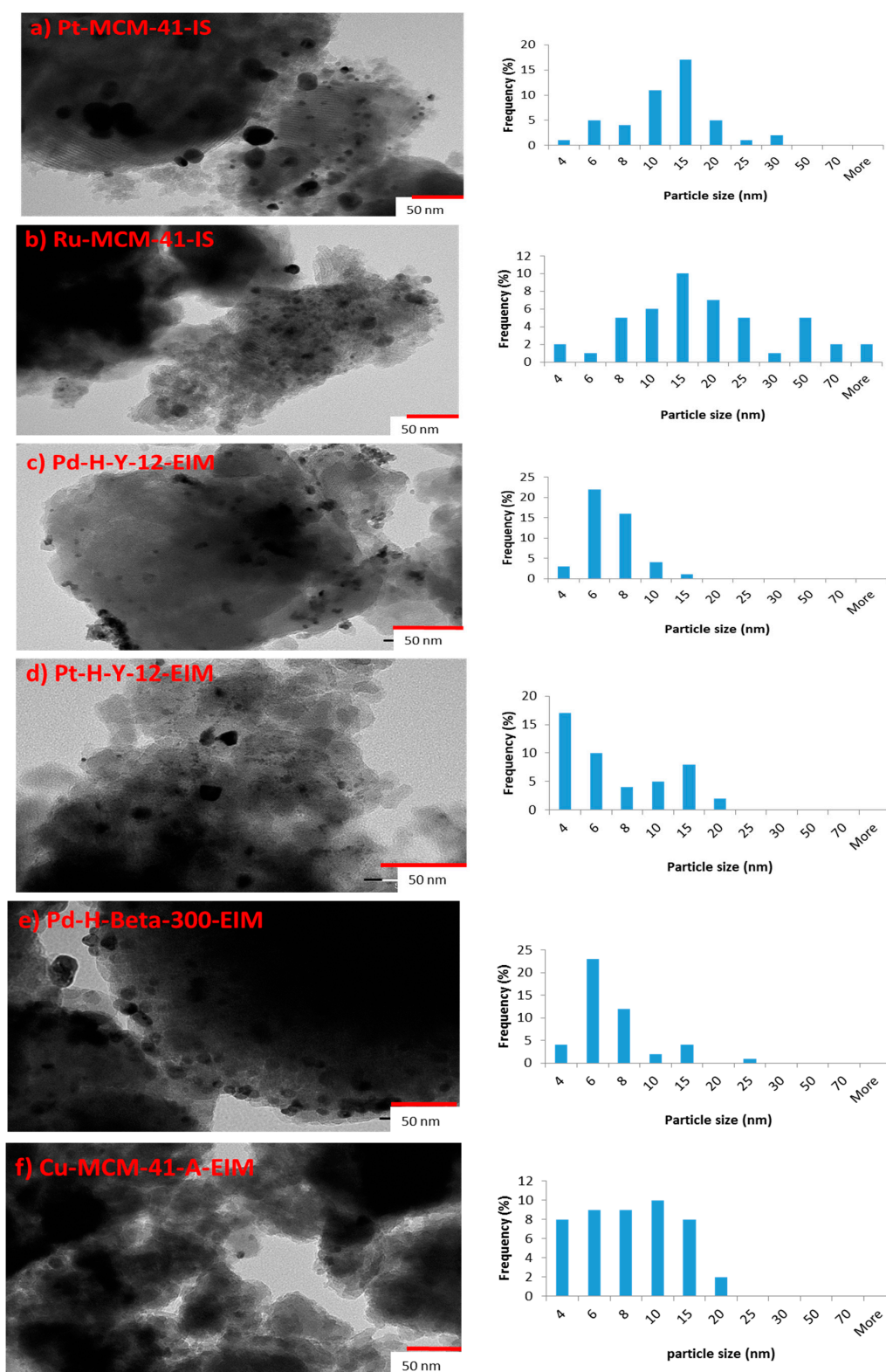
Figure 1. (**a**) TEM image and Pt particle size distribution histogram of Pt-MCM-41-IS, catalyst. (**b**) TEM image and Ru particle size distribution histogram of Ru-MCM-41-IS catalyst. (**c**) TEM image and Pd particle size distribution histogram of Pd-H-Y-12-EIM catalyst. (**d**) TEM image and Pt particle size distribution histogram of Pt-H-Y-12-EIM catalyst. (**e**) TEM image and Pd particle size distribution histogram of Pd-H-Beta-300-EIM catalyst. (**f**) TEM image and Cu particle size distribution histogram of Cu-MCM-41-A-EIM catalyst.

Table 1. Average cluster size distribution of Pt, Ru, Pd and Cu in the catalysts Pt-MCM-41-IS, Ru-MCM-41-IS, Pd-H-Y-12-EIM, Pt-H-Y-12-EIM, Pd-H-Beta-300-EIM and Cu-MCM-41-A-EIM.

Entry	Catalyst	Average Particle Size Distribution (nm)
1	Pt-MCM-41-IS	13.39
2	Ru-MCM-41-IS	13.29
3	Pd-H-Y-12-EIM	6.47
4	Pt-H-Y-12-EIM	5.72
5	Pd-H-Beta-300-EIM	6.11
6	Cu-MCM-41-A-EIM	7.82

The smallest average Pt particle sizes were measured for Pt-H-Y-12-EIM (5.72 nm), whereas the second smallest average Pd particle was measured for Pd-H-Beta-300-EIM (6.11 nm). The largest average particle size was observed for Pt-MCM-41-IS (13.395 nm). The mesoporous material Ru-MCM-41-IS catalyst synthesized also exhibited large average particles (13.29 nm).

It was concluded from the results of averages particle sizes (Table 1), that the method of introducing Pt-, Ru- into the mesoporous MCM-41 influenced the sizes of the particles. Hence, an in-situ method of introducing Pt- and Ru- resulted in large average particles sizes, once again confirming the significance of method of metal introduction in the MCM-41, mesoporous material.

For Cu-MCM-41-A-EIM, the mesoporous catalyst synthesized using the evaporation impregnation method, resulted in the average Cu particle size of 7.82 nm. Therefore, an introduction of metals (Pt-, Pd- and Cu-) using the evaporation impregnation method resulted in average smaller particle sizes.

2.1.2. Nitrogen Physisorption

The specific surface areas and specific pore volumes of fresh and spent Pt-, Ru and the Cu-MCM-41 mesoporous catalyst and Pd- and Pt-H-Y-12 catalysts were measured using nitrogen physisorption and results are collected in Table 2. The lowest specific surface area was obtained for the fresh Pt-MCM-41-IS (429 m^2/g) catalyst and this value increased after the catalyst had been used. The highest specific surface areas were determined for Pt-H-Y-12-EIM (857 m^2/g) and Pd-H-Beta-300-EIM (808 m^2/g).

Table 2. Specific surface area and pore volume of Pt-MCM-41-IS, Ru-MCM-41-IS, Pd-H-Y-12-EIM, Pt-H-Y-12-EIM, Pd-H-Beta-300-EIM and Cu-MCM-41-A-EIM catalysts applied in the experiments.

Entry	Catalyst	Specific Surface Area (m^2/g)		Pore Specific Volume (cm^3/g)	
		Fresh	Spent	Fresh	Spent
1	Pt-MCM-41-IS	429	555	0.409	0.552
2	Ru-MCM-41-IS	747	677	0.491	0.456
3	Pd-H-Y-12-EIM	667	732	0.237	0.259
4	Pt-H-Y-12-EIM	857	344	0.304	0.506
5	Pd-H-Beta-300-EIM	808	657	0.287	0.233
6	Cu-MCM-41-A-EIM	612	104	0.765	0.314

2.1.3. Scanning Electron Microscopy

The morphology, size and shape of the catalysts crystals were analyzed by scanning electron microscopy (SEM). The scanning electron micrographs of the Pt-MCM-41-IS, Ru-MCM-41-IS, Pd-H-Y-12-EIM, Pt-H-Y-12-EIM, Pd-H-Beta-300-EIM and Cu-MCM-41-A-EIM catalysts studied in the removal of CBZ from aqueous solutions exhibited a crystal morphology similar to that of H-MCM-41, H-Y-12 and H-Beta-300 catalyst, prior to their modifications with Pt-, Ru-, Pd- and Cu- metals. The crystal size distribution of the (a) Pt-MCM-41-IS, (b) Ru-MCM-41-IS, (c) Pd-H-Y-12-EIM, (d) Pt-H-Y-12-EIM, (e) Pd-H-Beta-300-EIM and (f) Cu-MCM-41-A-EIM in the form of histograms are displayed in Figure 2a–f. The average size of the catalyst crystals is presented in the Table 3. The largest average crystal size (272.45 nm) was obtained for the Pd-H-Beta-300-EIM synthesized

using evaporation impregnation. The second largest average crystal size measured for Pd-H-Y-12-EIM (257.12 nm) synthesized by using evaporation impregnation. The third largest average crystal size was measured for Pt-MCM-41-IS (219.23), prepared by the in-situ method. The explanation for the variations in the crystal sizes for synthesized catalysts is the structures of the H-Beta-300, H-Y-12 and MCM-41 mesoporous materials. Furthermore, the methods of the Pt-, Ru-, Pd- and Cu- introduction and the synthesis conditions can influence the average crystal size. The smallest crystal size (88.23 nm) was obtained for Cu-MCM-41-A-EIM, the catalyst synthesized using the evaporation impregnation method.
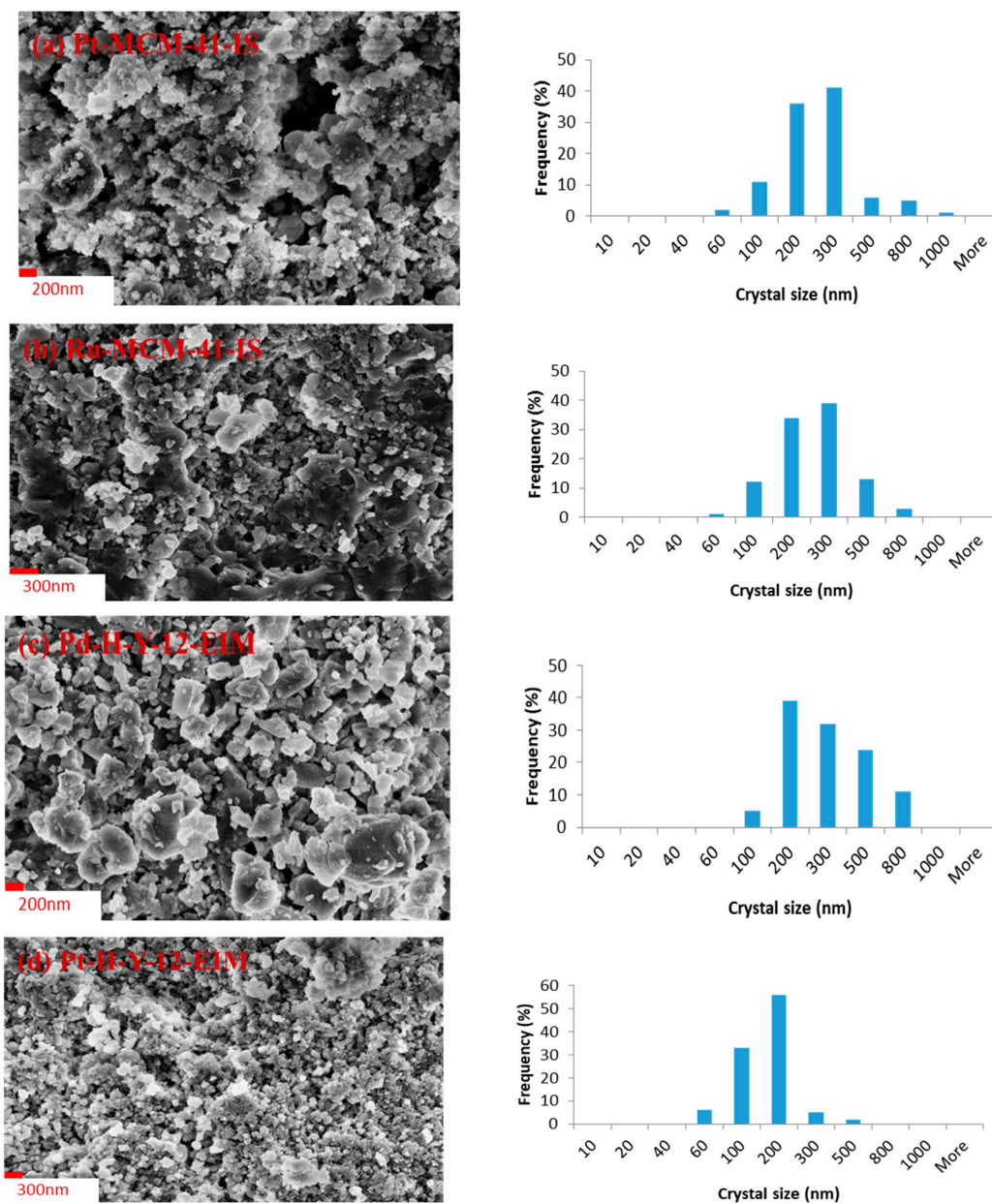

Figure 2. *Cont.*
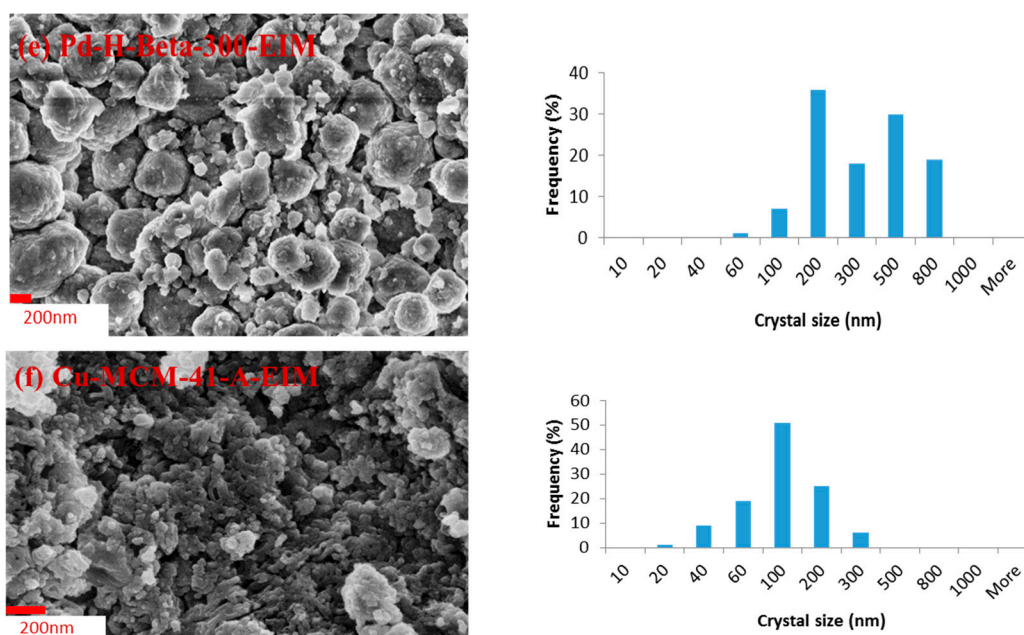
Figure 2. SEM image and crystal size distribution histogram of (**a**) Pt-MCM-41-IS. (**b**) Ru-MCM-41-IS catalyst. (**c**) Pd-H-Y-12-EIM. (**d**) Pt-H-Y-12-EIM. (**e**) Pd-H-Beta-300-EIM and (**f**) Cu-MCM-41-A-EIM catalysts.

Table 3. Average crystal size and metal (Pt, Ru, Pd and Cu) content of Pt-MCM-41-IS, Ru-MCM-41-IS, Pd-H-Y-12-EIM, Pt-H-Y-12-EIM, Pd-H-Beta-300-EIM and Cu-MCM-41-A-EIM catalysts.

Entry	Catalyst	Average Crystal Size (nm)	Metal Concentration (wt%)
1	Pt-MCM-41-IS	219.23	7.12
2	Ru-MCM-41-IS	202.39	1.55
3	Pd-H-Y-12-EIM	257.12	5.34
4	Pt-H-Y-12-EIM	119.62	1.67
5	Pd-H-Beta-300-EIM	272.45	1.95
6	Cu-MCM-41-A-EIM	88.23	3.46

2.1.4. Energy Dispersive X-ray Microanalysis

The Pt, Ru, Pd and Cu contents inside the Pt-MCM-41-IS, Ru-MCM-41-IS, Pd-H-Y-EIM, Pt-H-Y-12-EIM, Pd-H-Beta-300-EIM and Cu-MCM-41-A-EIM catalysts are given in Table 3. The highest amount of Pt was found for the Pt-MCM-41-IS catalyst. The largest amount of metal content (Pt) 7.12 wt% was measured for Pt-MCM-41-IS catalyst synthesized using the in situ method (Table 3). The Pd-H-Y-12-EIM catalyst synthesized using the evaporation method exhibited second highest metal (Pd) content 5.34 wt% Cu metal content (Table 3).

2.1.5. Pyridine Adsorption-Desorption with FTIR Spectroscopy

The concentration of Brønsted at 1545 cm^{-1} and Lewis at 1450 cm^{-1} acid sites were measured with FTIR using pyridine as a probe molecule. At 250–350 °C, pyridine desorption demonstrate weak, medium and strong sites, whereas at 350–450 °C it exhibited medium and strong sites and finally at 450 °C, strong sites prevailed. The acidity of the Pt-MCM-41-IS, Ru-MCM-41-IS, Pd-H-Y-12-EIM, Pt-H-Y-12-EIM, Pd-H-Beta-300-EIM and Cu-MCM-41-A-EIM catalysts analyzed via FTIR is listed in Table 4. Following that, the data of the determination were converted into concentrations using the extinction coefficients of Emeis [33]. It was noticed that Pd-H-Y-EIM showed the presence of largest Brønsted acidity (237 µmol/g) at 250 °C compared to other catalyst. The catalysts Cu-MCM-41-EIM and

Pd-H-Y-12-EIM catalysts had higher Lewis acidities (56 μmol/g and 52 μmol/g) at 250 °C, compared to the other catalysts.

Table 4. Brønsted and Lewis acidities of Pt-MCM-41-IS, Ru-MCM-41-IS, Pd-H-Y-12-EIM, Pt-H-Y-12-EIM, Pd-H-Beta-300-EIM and Cu-MCM-41-A-EIM catalysts.

Catalysts	Brønsted Acidity (μmoL/g)			Lewis Acidity (μmoL/g)		
	250 °C	350 °C	450 °C	250 °C	350 °C	450 °C
Pt-MCM-41-IS	7	2	0	1	1	0
Ru-MCM-41-IS	18	0	0	9	0	0
Pd-H-Y-12-EIM	237	24	0	52	6	0
Pt-H-Y-12-EIM	96	28	0	3	13	0
Pd-H-Beta-300-EIM	58	18	0	9	7	0
Cu-MCM-41-A-EIM	44	10	0	56	9	0

2.1.6. Characterization by X-ray Photoelectron Spectroscopy

The surface composition and oxidation state of metals were determined by the X-ray photoelectron spectroscopy (XPS) method. The XPS analysis indicated the oxidation states of Pt° and PtO on the Pt-MCM-41-IS catalyst (Figure 3a) Similarly oxidation state of Pt in the Pt-H-Y-12-EIM was measured as Pt, PtO_2 (Figure 3d). The oxidation states of Ru in Ru-MCM-41-IS was determined as Ru° and RuO_2 (Figure 3b). The oxidation states of Pd in Pd-H-Y-12-EIM and Pd-H-Beta-300-EIM were measured to be Pd° (Figure 3c,e). The oxidation state of Cu in Cu-MCM-41-A-EIM was measured to be Cu° and CuO (Figure 3f).
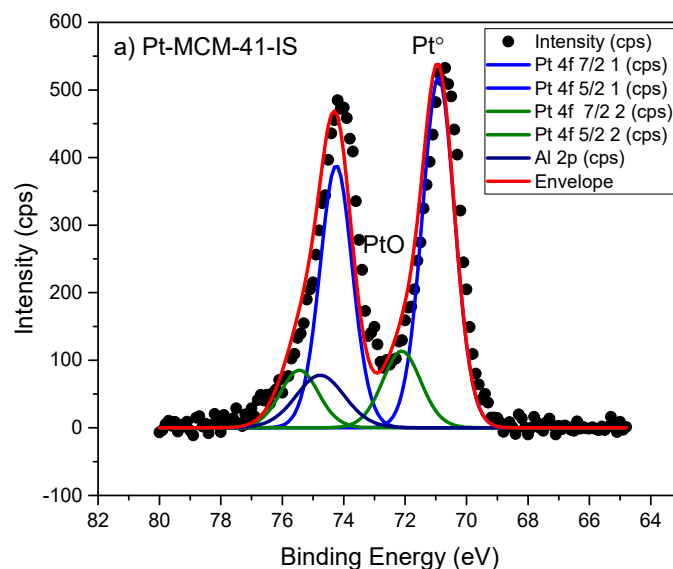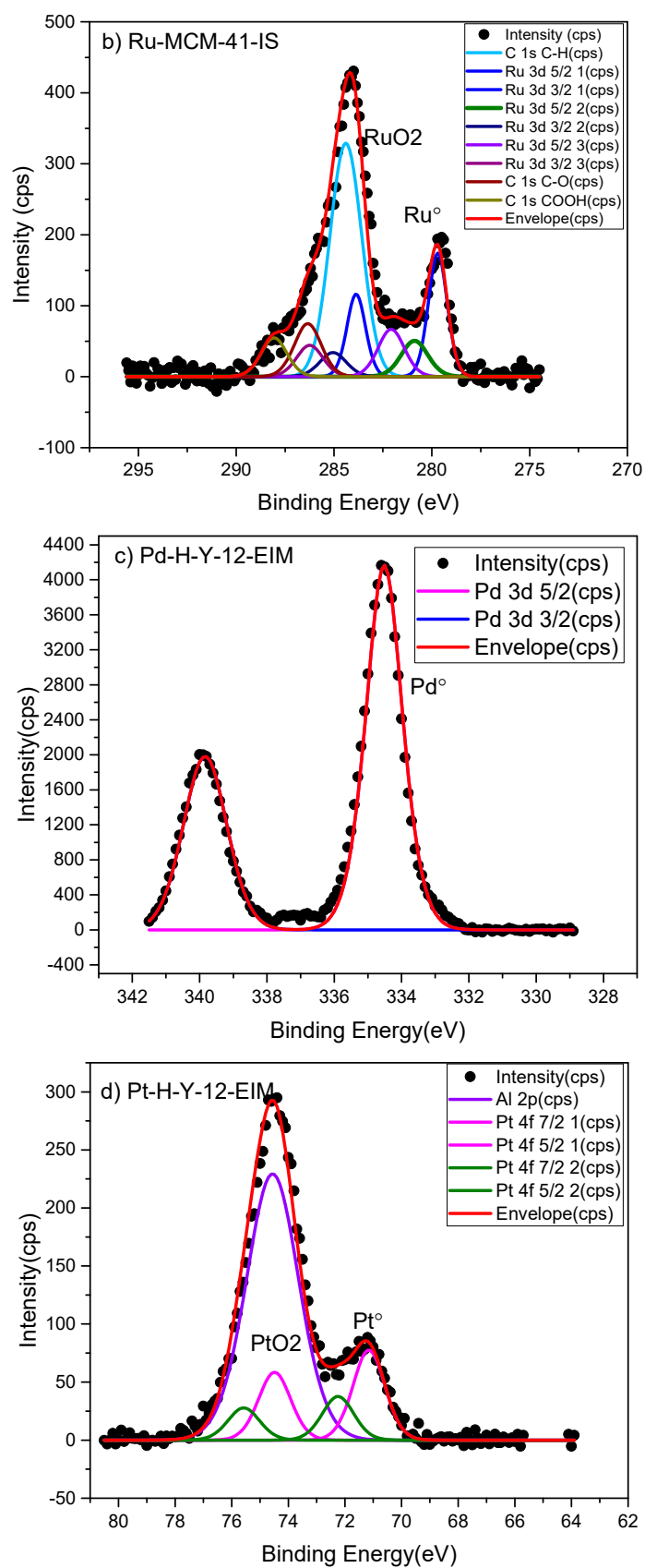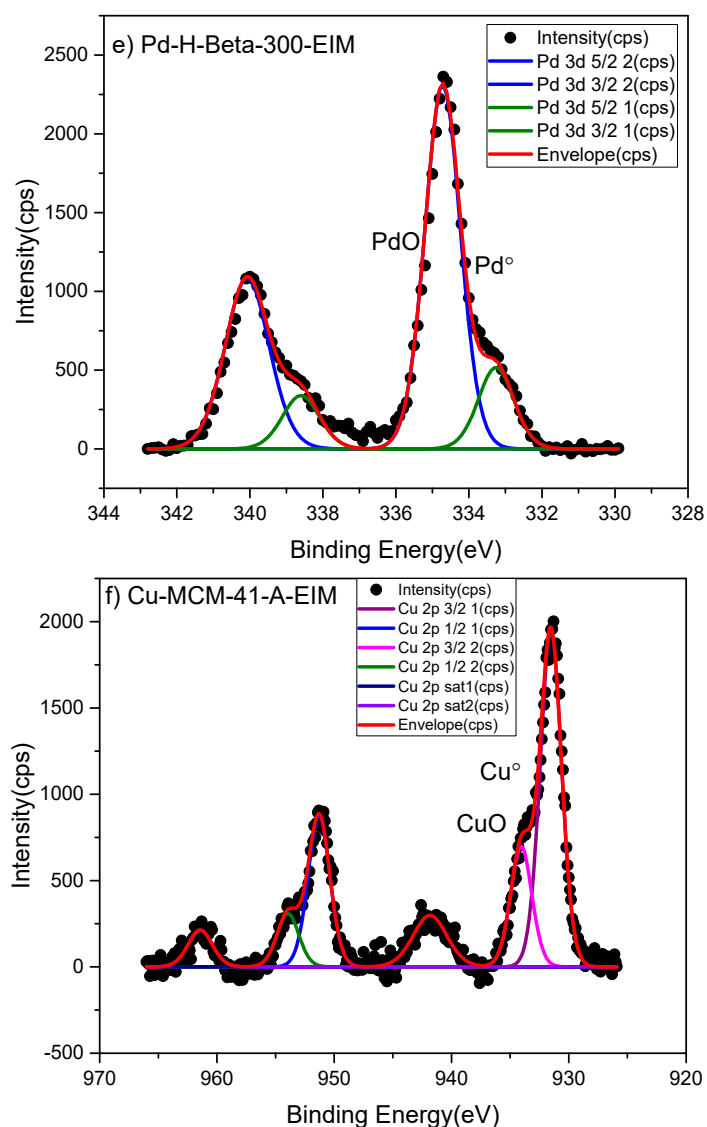

Figure 3. *Cont.*

Figure 3. *Cont.*

Figure 3. X-ray photoelectron spectroscopy (XPS) spectra of (**a**) Pt-MCM-41-IS, (**b**) Ru-MCM-41-IS, (**c**) Pd-H-Y-12-EIM, (**d**) Pt-H-Y-12-EIM, (**e**) Pd-H-Beta-300-EIM and (**f**) Cu-MCM-41-A-EIM catalysts.

2.2. Non-Catalytic and Catalytic Ozonation of Carbamazepine

2.2.1. Influence of Different Catalysts in the Degradation of Carbamazepine and its By-Products in the Presence of Ozone

The influence of different temperatures (5 °C, 20 °C and 50 °C) on the ozonation of CBZ on the reaction rate was evaluated the results are displayed in Figure 4a. These experiments illustrate that the transformation rate of CBZ was rapid and approximately equal to each other, at these three temperatures. After 5 min of ozonation, all the CBZ was transformed. Somathilake et al. obtained similar results from the ozonation of CBZ [34]. The degradation kinetics of CBZ by 0.5 g/L of Pd-H-Beta-300-EIM was studied in the absence and presence of ozone (Figure 4b). This experiment revealed that the CBZ concentration did not change in the absence of ozone, which indicates that the catalyst does not absorb CBZ and it is not transformed without the presence of ozone.
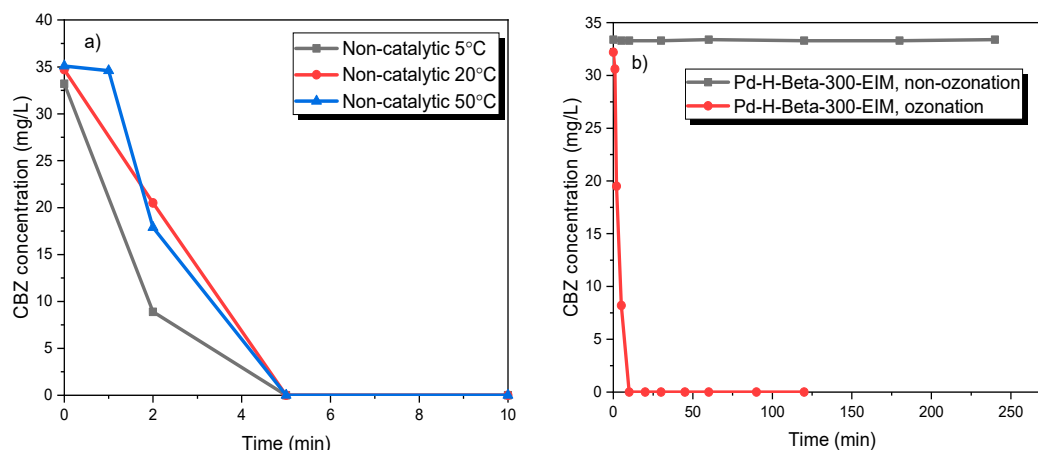
Figure 4. (**a**) CBZ degradation by ozonation at different temperatures (5 °C, 10 °C, 20 °C and 50 °C). (**b**) CBZ degradation by catalysis in the presence and absence of ozone at temperature 20 °C (stirring speed = 900 rpm, $C_{O3,g}$ = 21 mg/L, C_{CBZ} = 35 mg/L, gas flow rate = 110 mL/min, $C_{catalysts}$ = 0.5 g/L).

An identical series of catalytic ozonation experiments were conducted at 20 °C in order to evaluate the effect of different heterogeneous catalysts on the degradation rate of CBZ. Figure 5a shows that Cu-MCM-41-A-EIM and Ru-MCM-41-IS showed higher degradation rates compared to other catalysts the conversion of CBZ was complete already after two minutes for the Cu-catalyst and the Ru-catalyst was almost as active.
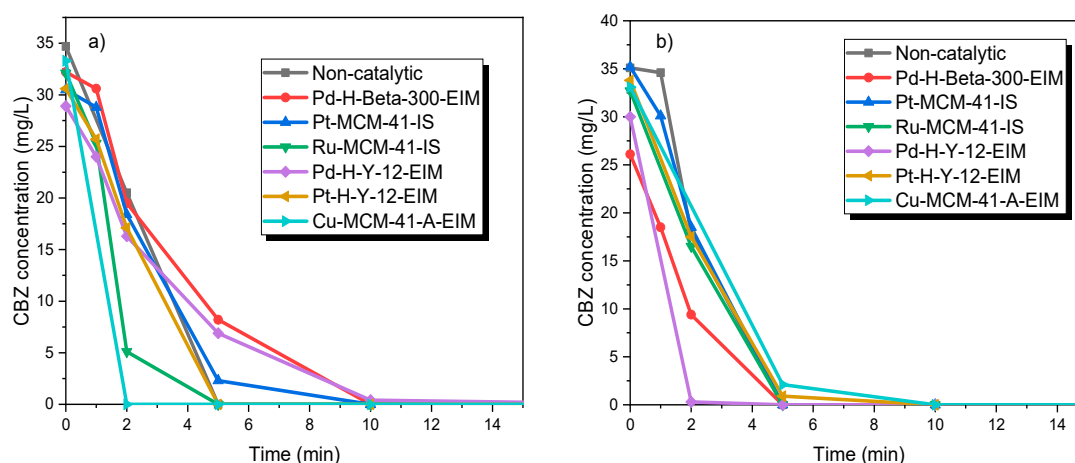

Figure 5. CBZ degradation by ozonation and ozonation combined with catalysis. C_{CBZ} = 35 mg/L, gas flow rate = 110 mL/min, stirring speed = 900 rpm, $C_{O3, g}$ = 21 mg/L, $C_{catalysts}$ = 0.5 g/L. (**a**) T = 20 °C and (**b**) T = 50 °C.

A similar series of catalytic ozonation experiments were carried out at 50 °C, to evaluate the effect of increased temperature on the catalyst activity while ozonating CBZ (Figure 5b). As revealed in our previous work, the dissolved ozone concentration decreases at higher temperature but, on the other hand, the activity of catalysts increases at higher temperature [31,35]. Here, the Pd-H-Y-12-EIM and Pd-H-Beta-300-EIM illustrated the highest decomposition rate compared to other catalysts and the non-catalytic experiment. Due to the rapid reaction rate, it is hard to evaluate the temperature effect on decomposition rate of CBZ.

2.2.2. Quantification of Catalytic and Non-Catalytic Ozonation Products

Han et al. studied [36] cytotoxicity and genotoxicity of the removal CBZ through chlorination, chloro-amination and ozonation processes. The CBZ solely induces chromosomal damage, and on the other hand, the genotoxicity of the CBZ residues after each treatment was found to be higher. Moreover,

it was demonstrated that the most efficient way for the degradation of CBZ was by ozonation among the other treatments. However, the by-products formed by ozonation exhibited the highest cytotoxicity and an elevated genotoxicity. The authors suspected that the by-products BQM and BQD might cause chromosomal damage effects.

The main ozonation pathway of CBZ is a rapid, almost instantaneous reaction leading to BQM (Figure 6). BQM is transformed further slowly to BQD [37]. In order to investigate the effect of heterogeneous catalysts on the formation and transformation of BQM and BQD, the products were isolated from the kinetic experiments and a quantification method was developed.

Figure 6. CBZ and its main ozonation products.

The temperature effect on the formation of by-products was also studied for the non-catalytic ozonation using the same temperatures as above. The influence of the reactor temperature on the ozonation of CBZ into BQM and BQD is illustrated in Figure 7. It can be noticed that at higher temperature (50 °C), the concentration of BQM remained at a high level and after 4 h it had only decreased to 19.5 mg/L from the highest value of 28 mg/mL. At lower temperatures (20 °C and 5 °C), the reaction proceeded more rapidly, and almost all of BQM was removed or transformed after four hours. The concentration of the secondary by-product BQD increased simultaneously to 20–24 mg/L when performing the experiments at low temperature (5–20 °C), but it remained low at the higher temperature (50 °C), due to a slow transformation of BQM, BQD formed slower at higher temperatures. If the experiment at 50 °C had been continued, the concentration of BQD might have been the same as for the experiments at lower temperatures. It can be concluded that by lowering the temperature due to higher dissolved ozone concentration, CBZ rapidly converts to BQM, and later on it transforms to BQD faster than at the higher temperature (50 °C).

Figure 7. (**a**) BQM and (**b**) BQD concentration during the ozonation of CBZ. C_{CBZ} = 35 mg/L, gas flow rate = 110 mL/min, T = 5 °C, 10 °C, 20 °C and 50 °C, stirring speed = 900 rpm, $C_{O3, g}$ = 21 mg/L.

Thereafter, several solid catalysts, which were synthesized and characterized by our group, were employed to reveal the catalytic effect on the CBZ. The formation kinetic of BQM and BQD are displayed in Figures 8 and 9. It was observed that during the first minutes of experiments, the BQM

concentration increased to a maximum 25.7 mg/L (Cu-MCM-41-A-EIM), later on it decreased in 2 h to a minimum of 4 mg/L. For non-catalytic ozonation at 20 °C, the BQM concentration increased to 25.7 mg/L but after 2 h it decreased to 4.8 mg/L. Pt-H-Y-12-EIM and Ru-MCM-41-IS catalysts showed a slightly higher transformation rate of BQM compared to the corresponding non-catalytic experiment. As revealed by Figure 9, BQD was slightly formed within 2 h. The maximum concentration of BQD was 20.2 mg/L for non-catalytic experiment. The catalyst Pd-H-Y-12-EIM showed the lowest BQD concentration (1.7 mg/L) also Pd-H-Beta-300 showed lower formation of BQD (11.9 mg/L). Three mechanisms could occur in these experiments, (1) ozone adsorption on the catalyst surface and generation of active radical species that react with BQM and BQD; (2) BQM and BQD sorption on the catalyst surface followed via the reaction by dissolved ozone in the water and (3) sorption of all three species ozone, BQM and BQD on the catalyst surface followed by a direct or indirect reaction [38].
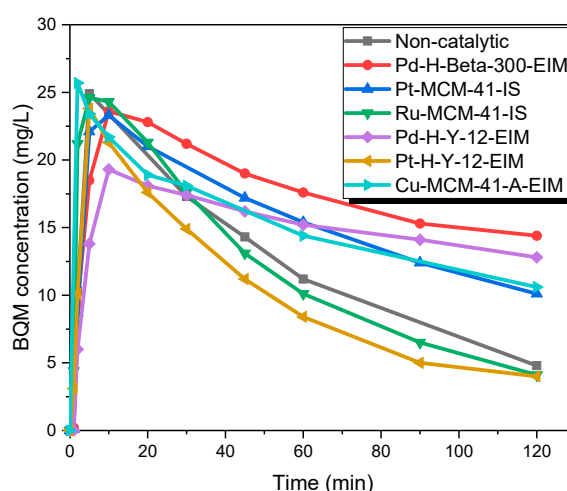
Figure 8. BQM concentration during the catalytic and non-catalytic ozonation of CBZ. C_{CBZ} = 35 mg/L, gas flow rate = 110 mL/min, T = 20 °C, stirring speed = 900 rpm, $C_{O3,g}$ = 21 mg/L, $C_{catalysts}$ = 0.5 g/L.
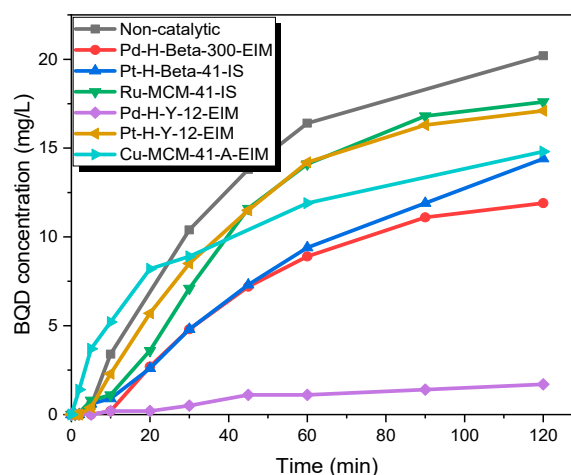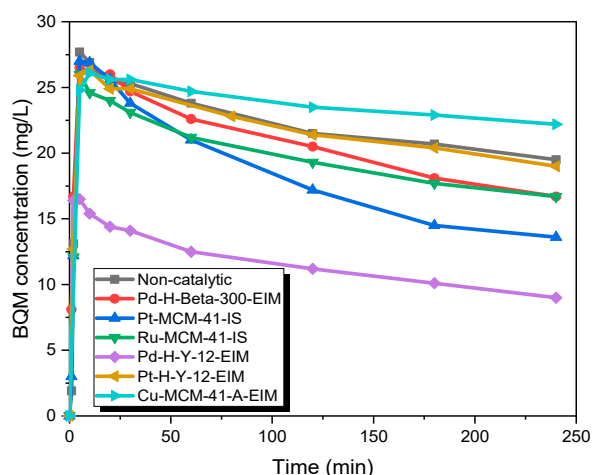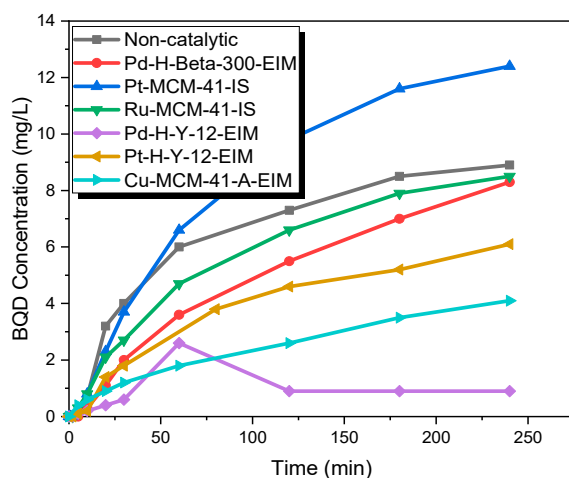

Figure 9. BQD concentration during the catalytic and non-catalytic ozonation of CBZ. C_{CBZ} = 35 mg/L, gas flow rate = 110 mL/min, T = 20 °C, stirring speed = 900 rpm, $C_{O3,g}$ = 21 mg/L, $C_{catalysts}$ = 0.5 g/L.

The catalytic experiments were carried out under several temperatures. Figure 10 shows that in the first minutes, 27.7 mg/L of BQM was formed (similar to non-catalytic ozonation), but later on, the BQM concentration slightly decreased to 9 mg/L when using the Pd-H-Y-12-EIM catalyst. For non-catalytic ozonation at 50 °C, the BQM concentration increased to 27.7 mg/L, after which it decreased to 21.4 after 2 h, and after 4 h it had decreased to 19 mg/L. It can be noticed from results that the activity of catalyst increased with higher temperature, since dissolved ozone concentration is

very low at 50 °C (approximately five times lower than at 20 °C). For example, after 2 h of ozonation combined with Pd-H-Y-12-EIM catalyst, the BQM and BQD concentration were 11.2 mg/L and 0.9 at 50 °C, which were lower compared to 20 °C (BQM concentration was 12.8 mg/L and BQD concentration was 1.7 mg/L) with the same catalyst (Figure 11). One explanation for the increased catalytic efficiency at higher temperatures could be due to that instead of ozonation, catalytic oxidation is observed, where dissolved oxygen is adsorbed on metal oxides and the further generate active atomic oxygen species as well as lattice oxygen atoms, which are present on the metal oxides of catalysts [39].

Figure 10. BQM concentration during the catalytic and non-catalytic ozonation of CBZ. C_{CBZ} = 35 mg/L, gas flow rate = 110 mL/min, T = 50 °C, stirring speed = 900 rpm, $C_{O3,g}$ = 21 mg/L, $C_{catalysts}$ = 0.5 g/L.

Figure 11. BQD concentration during the catalytic and non-catalytic ozonation of CBZ. C_{CBZ} = 35 mg/L, gas flow rate = 110 mL/min, T = 50 °C, stirring speed = 900 rpm, $C_{O3,g}$ = 21 mg/L, $C_{catalysts}$ = 0.5 g/L.

These results were in line with a study performed by Rosal et al. who investigated catalytic ozonation of CBZ. Their ozonation results revealed that utilizing a titanium dioxide catalyst combined with ozonation provides a significant benefit where the ozone decomposition as well as ozonation reactions were improved, as well as an increase of the formation of hydroxyl radicals and rate of mineralization compared to non-catalytic ozonation [40].

A more detailed investigation of the fate of BQD was conducted using isolated BQD without CBZ and other by-products. Pure BQD was obtained by isolation from an ozonation experiment. BQD was dissolved in acetonitrile and deionized water. Non-catalytic and catalytic ozonation was carried out with this solution. Figure 12 demonstrates that after 4 h of non-catalytic ozonation only 6% of BQD

remained and after 4 h catalytic ozonation only 3% of BQD, catalytic ozonation slightly increased transformation rate.
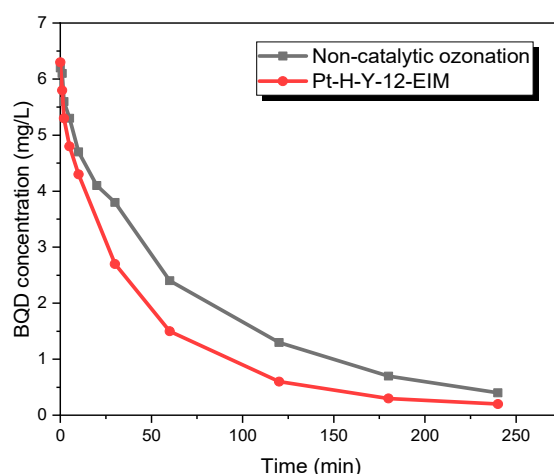

Figure 12. BQD concentration during the catalytic and non-catalytic ozonation of BQD. C_{BQD} = 6 mg/L, $C_{Acetonitrile}$ = 6 mg/L, gas flow rate = 110 mL/min, T = 50 °C, stirring speed = 900 rpm, $C_{O3,g}$ = 21 mg/L, $C_{catalysts}$ = 0.5 g/L.

2.2.3. Leaching of Modified Metals and Aluminum from Catalysts

Inductively coupled optical emission spectrometry (ICP-OES) Optima 5300 DV Perkin Elmer instrument was applied to determine leaching of catalytic metals during ozonation at 20 °C. The aluminum and modified metal were considered in these experiments. Cu-MCM-41A-EIM catalyst showed high leaching of Cu 58.9% and Pd-H-Beta-300-EIM relatively high leaching of Pd and aluminum 14.2% and 20.26% respectively. On the contrary, Pt-H-Y-12-EIM, Ru-MCM-41-IS, Pt-MCM-41-IS showed no leaching for modified metal. Figure 13 illustrates the catalyst leaching during 2 h ozonation.
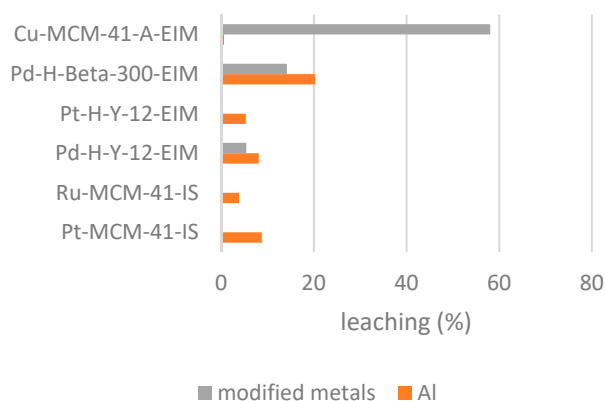

Figure 13. Leaching of modified metal and aluminum (%) in the catalytic ozonation of CBZ at 20 °C.

3. Materials and Methods

3.1. Chemicals

Carbamazepine (CBZ; $C_{15}H_{12}N_2O$, MW: 236.269 g/mol, CAS number: 298-46-4) was purchased from Sigma Life Science. The CBZ was in crystal powder form, therefore it was first dissolved in methanol (H_3COH, MW: 32.04 g/mol, CAS number: 67-56-1), which was obtained from VWR (Briare, France). The water used in the LC-MS analysis was purified using a Millipore Simplicity 185 system (Millipore S.A.S., Molsheim, France). The acetonitrile used in the LC-MS analysis was of LC-MS grade

and was obtained from Fisher scientific and formic acid was obtained from Sigma-Aldrich. BQM and BQD were prepared from ozonation following to the procedure Kråkström et al. Stock solutions of BQM and BQD were prepared in acetonitrile.

3.2. Catalyst Preparation

The following solid catalysts were prepared in our laboratory: Pt-MCM-41-IS, Ru-MCM-41-IS, Pd-H-Y-12-EIM, Pt-H-Y-12-EIM, Pd-H-Beta-300-EIM and Cu-MCM-41-A-EIM. The Pt and Ru modification of Pt-MCM-41-IS and Ru-MCM-41-IS was carried out using the in-situ (IS) synthesis preparation method [41]. The modification methods for Pd, Pt and Cu used for the synthesis of Pd-H-Y-12-EIM, Pt-H-Y-12-EIM, Pd-H-Beta-300-EIM and Cu-MCM-41-A-EIM catalysts were evaporation impregnation (EIM) [31].

For the synthesis of Pd-H-Y-12-EIM, an aqueous solution of $Pd(NO_3)_2$ and H-Y-12 was placed in a Rotavapor for 24 h, until the aqueous phase was evaporated at 60 °C. The Pd-H-Y-12-EIM catalyst was transferred from the flask and dried in an oven overnight at 100 °C. Finally, it was calcined in a muffle oven at 450 °C for three hours.

3.3. Physico-Chemical Characterization of Catalyst

The electron micrographs, metal particle size and structural properties of the catalysts were investigated by transmission electron microscopy (TEM, model JEM 1400 plus: Jeol Ltd., Tokyo, Japan) using a transmission electron microscope (model JEM 1400 Plus), using 120 kV accelerating voltage and a resolution of 0.38 nm provided via OSIS Quemesa 11 Mpix digital camera (rephrase/split). The specific surface areas and pore volumes of the catalysts were determined by nitrogen physisorption (Carlo Erba Sorptomatic 1900, Fisons Instruments, Milan, Italy) and interpreted with Dubinin and B.E.T. (Brunauer–Emmett–Teller) equations. The fresh catalysts were outgassed at 150 °C, whereas the spent catalysts were outgassed at 100 °C for 3 h before each and every nitrogen adsorption measurement. Scanning electron microscopy coupled to energy disperse X-ray analysis (SEM/EDXA) was used to investigate morphology. Crystallite size and metal contents of catalysts was analyzed by SEM (Zeiss Leo Gemini 1530, Oberkochen, Germany) and energy dispersive X-ray micro-analysis. The catalyst acidities were measured by Fourier transform infrared spectroscopy (FTIR) spectroscopy (ATI Mattson Infinity series, Madison, MI, USA) by employing pyridine as the probe molecule. The X-ray photoelectron spectroscopy (XPS, Kratos Analytical, UK) analysis was performed using an X-ray spectrometer (lens mode hybrid resolution by mono aluminum). The specific elemental analysis was done using 20 eV pass energy.

3.4. Kinetic Experiments in a Semi-Batch Reactor

The ozonation experiments were conducted in a double jacket isothermal glass reactor operating in semibatch mode. In order to immobilize the solid catalyst used in these experiments, a Spinchem ^{TM} rotating bed reactor (RBR) was used, typically operating at 900 rpm to ensure vigorous mixing of the liquid and gas phases and to maximize the mass transfer between the gas–liquid interface and the solid catalyst surface. An ozone generator (Absolute Ozone, Nano model, Edmonton, AB, Canada) was used to provide ozone, using oxygen (108.5 mL/min) and nitrogen (1.5 mL/min) as the gas flow rate to the generator was, so the total gas flow was 110 mL/min. The feed gas was super-dried (dew point −60 °C). The ozonator produced a concentration of approximately 21 mg/L of ozone in the gas phase. The ozone concentration was determined by iodine volumetric titration [42]. In order to purge the gas constantly through the reactor vessel, a 7 μm disperser was used at the bottom of the reactor. The dissolved ozone concentration was determined to 1.668 mg/L at 5 °C, 0.441 mg/L at 20 °C and 0.0921 mg/L at 50 °C by the indigo method. The water solubility of CBZ is rather low, only 17.7 mg/L, while it is fully soluble in methanol. Therefore, the stock solution was prepared by dissolving 0.35 g CBZ in 100 mL of methanol. Thereafter, 10 mL of the stock solution was added to 1 L deionized water in the glass reactor in the beginning of each experiment. The initial concentration of CBZ was thus 35 mg/L, which is higher than

the concentration typically detected in surface waters. However, a high initial concentration allows us to detect and identify by-products of very low concentrations. In this study, the reaction time was varied from 180 to 240 min. The reactor system used in the experiments is displayed in Figure 14.
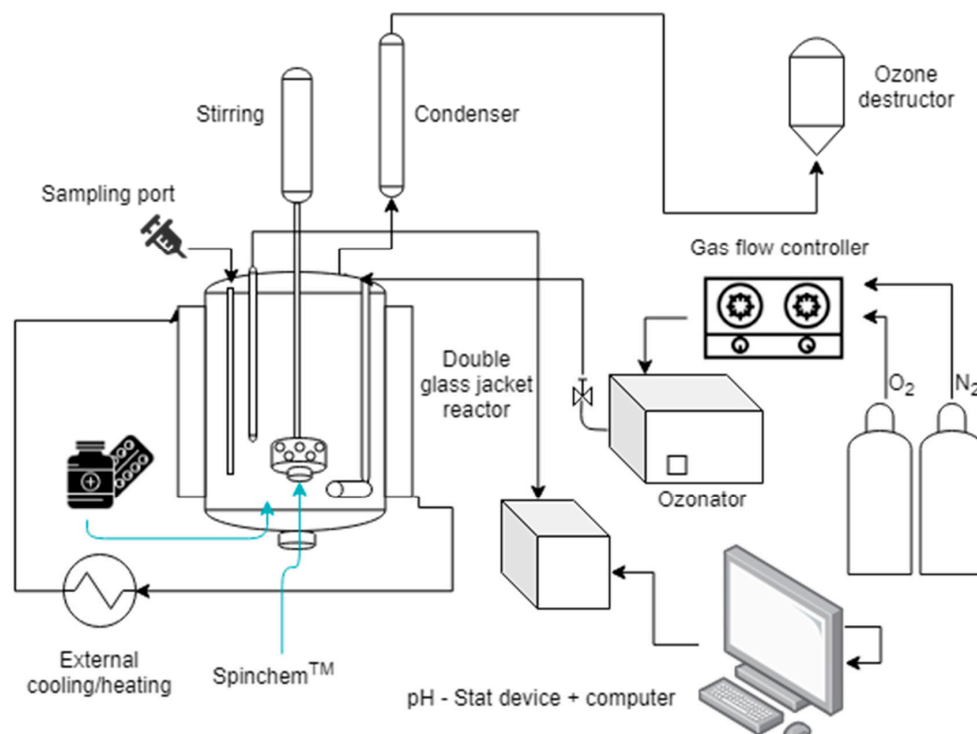

Figure 14. Schematic view of the semi-batch reactor system for degradation of CBZ.

3.5. Quantification of CBZ, BQM and BQD

Various systems have been developed for the analysis and determination of CBZ such as liquid chromatography-mass spectrometry (LC-MS) and gas chromatography-mass spectrometry (GC-MC) [43,44]. For quantification, an Agilent 1100 LC system equipped with a variable wavelength detector set to 254 nm was used. The chromatographic separation was performed using an Agilent 1100 binary pump equipped with a vacuum degasser, an autosampler and a thermostated column oven set to 30 °C and a Waters Atlantis T3 C18 column (2.1 × 100 mm, 3 µm). The eluents were 0.1% formic acid in water (A) and 0.1% formic acid in acetonitrile (B). Initially the composition was held at 0% (B) for 1 min, then the composition was increased linearly to 30% (B) over 9 min. The composition was further increased linearly to 95% (B) over 14 min. Finally, the eluent composition was returned to the initial conditions over the next 1 min and given 10 min for equilibration. The flow rate was 0.3 mL/min. The injection volume was 30 µL. The draw speed was 100 µL/min while the eject speed was 100 µL/min. Using the stock solutions, calibration curves consisting of eight points (in water) were prepared separately for CBZ, BQM and BQD. The ozonated samples were analyzed without any further adjustment.

An MSD ion trap mass spectrometer equipped with an electrospray ionization (ESI) source operating in full scan mode was used for confirmation of the structure. Nitrogen was used as drying gas and argon was used as collision gas. The drying gas was held at 8 L/min and heated to 350 °C. The nebulizer pressure was set to 40 psi. The scan range was set to 50–600 m/z.

4. Conclusions

The current work demonstrated the degradation kinetics of CBZ by ozonation at two reaction temperatures (20 °C and 50 °C), and a number of zeolite catalysts. Pt-MCM-41-IS,

Ru-MCM-41-IS, Pd-H-Y-12-EIM, Pt-H-Y-12-EIM, Pd-H-Beta-300-EIM and Cu-MCM-41-A-EIM catalysts were synthesized and applied with combination of ozone for the removal of CBZ and its ozonation transformed products. Several experiments were carried out in order to evaluate the influence of temperature on the catalyst activity. By increasing the reactor temperature to 50 °C the activities of the catalysts increased, even though the dissolved ozone concentration decreased dramatically at 50 °C compared to 20 °C. The formation of the products BQM and BQD were kinetically displayed and the role of the catalysts were discussed. CBZ rapidly transformed into BQM and later into BQD. The by-product analysis illustrated that degradation of BQM and BQD was higher when using a catalyst combined with ozonation. In addition, Pd-H-Y-12-EIM prepared by evaporation impregnation method revealed the highest degradation rate of BQM and BQD compared to other catalysts at 50 °C. The catalyst Pd-H-Y-12-EIM had the highest Brønsted acidity 237 µmol/g at 250 °C and moderately high Lewis acidity 52 µmol/g at 250 °C. This indicates that the acidity of catalyst has a big role in the transformation of CBZ. Moreover, this catalyst had a high average crystal size, 257.11 nm, compared to the other catalysts, and the Pd concentration was relatively large, 5.34 wt%. The leaching was relatively low for Pd and Al for this catalyst, which makes it a promising catalyst for the ozonation of pharmaceuticals of this kind.

Author Contributions: M.K. and S.S. are Ph.D. students, senior scientists and supervisors with the following competences: P.T.: ozonation technology, N.K.: catalyst specialist, K.E.: reactor design, T.S.: chemical kinetics and experimental planning, J.-P.M.: stirrer expert, L.K.: analysis of organic components in aqueous environment, P.E.: organic reaction technology, M.P.: TEM expert, A.A.: FTIR expert, A.S.: XPS expert. All authors have read and agreed to the published version of the manuscript.

Conflicts of Interest: The authors declare no competing financial interest.

References

1. Ying, G.-G.; Jiang, Y.-X.; Yang, Y.-Y.; Yao, L.; Zhang, J.-N.; Liu, W.-R.; Zhao, J.-L.; Zhang, Q.-Q.; Liu, Y.-S.; Hu, L.-X. Pharmaceuticals and personal care products (PPCPs) and artificial sweeteners (ASs) in surface and ground waters and their application as indication of wastewater contamination. *Sci. Total Environ.* **2017**, *616–617*, 816–823. [CrossRef]

2. Tran, N.H.; Reinhard, M.; Gin, K.Y.H. Occurrence and fate of emerging contaminants in municipal wastewater treatment plants from different geographical regions-a review. *Water Res.* **2018**, *133*, 182–207. [CrossRef] [PubMed]

3. D'Alessio, M.; Onanong, S.; Snow, D.D.; Ray, C. Occurrence and removal of pharmaceutical compounds and steroids at four wastewater treatment plants in Hawai'i and their environmental fate. *Sci. Total Environ.* **2018**, *631–632*, 1360–1370.

4. Tarpani, R.R.Z.; Azapagic, A. A methodology for estimating concentrations of pharmaceuticals and personal care products (PPCPs) in wastewater treatment plants and in freshwaters. *Sci. Total Environ.* **2018**, *622–623*, 1417–1430. [CrossRef]

5. Papageorgiou, M.; Kosma, C.; Lambropoulou, D. Seasonal occurrence, removal, mass loading and environmental risk assessment of 55 pharmaceuticals and personal care products in a municipal wastewater treatment plant in Central Greece. *Sci. Total Environ.* **2016**, *543*, 547–569. [CrossRef]

6. Fu, Q.; Han, Y.; Xie, Y.F.; Gong, N.B.; Guo, F. Carbamazepine cocrystals with several aromatic carboxylic acids in different stoichiometries: Structures and solid state characterization. *J. Mol. Struct.* **2018**, *1168*, 145–152. [CrossRef]

7. World Health Organization. *WHO Model List of Essential Medicines*, 20th ed.; WHO: Geneva, Switzerland, 2017.

8. Ekpeghere, K.I.; Sim, W.J.; Lee, H.J.; Oh, J.E. Occurrence and distribution of carbamazepine, nicotine, estrogenic compounds, and their transformation products in wastewater from various treatment plants and the aquatic environment. *Sci. Total Environ.* **2018**, *640–641*, 1015–1023. [CrossRef]

9. Wang, J.; Wang, S. Removal of pharmaceuticals and personal care products (PPCPs) from wastewater: A review. *J. Environ. Manag.* **2016**, *182*, 620–640. [CrossRef]

10. Björlenius, B.; Ripszám, M.; Haglund, P.; Lindberg, R.H.; Tysklind, M.; Fick, J. Pharmaceutical residues are widespread in Baltic Sea coastal and offshore waters—Screening for pharmaceuticals and modelling of environmental concentrations of carbamazepine. *Sci. Total Environ.* **2018**, *633*, 1496–1509. [CrossRef]

11. Fattore, E.; Zuccato, E.; Castiglioni, S.; Davoli, E.; Riva, F. Risk assessment of a mixture of emerging contaminants in surface water in a highly urbanized area in Italy. *J. Hazard. Mater.* **2018**, *361*, 103–110.

12. Radović, T.; Grujić, S.; Petković, A.; Dimkić, M.; Laušević, M. Determination of pharmaceuticals and pesticides in river sediments and corresponding surface and ground water in the Danube River and tributaries in Serbia. *Environ. Monit. Assess.* **2015**, *187*, 4092. [CrossRef] [PubMed]

13. Bahlmann, A.; Brack, W.; Schneider, R.J.; Krauss, M. Carbamazepine and its metabolites in wastewater: Analytical pitfalls and occurrence in Germany and Portugal. *Water Res.* **2014**, *57*, 104–114. [CrossRef] [PubMed]

14. Jurado, A.; López-Serna, R.; Vázquez-Suné, E.; Carrera, J.; Pujades, E.; Petrovic, M.; Barceló, D. Occurrence of carbamazepine and five metabolites in an urban aquifer. *Chemosphere* **2014**, *115*, 47–53. [CrossRef] [PubMed]

15. Brezina, E.; Prasse, C.; Meyer, J.; Mückter, H.; Ternes, T.A. Investigation and risk evaluation of the occurrence of carbamazepine, oxcarbazepine, their human metabolites and transformation products in the urban water cycle. *Environ. Pollut.* **2017**, *225*, 261–269. [CrossRef]

16. Wang, S.; Wang, J. Degradation of carbamazepine by radiation-induced activation of peroxymonosulfate. *Chem. Eng. J.* **2018**, *336*, 595–601. [CrossRef]

17. Almeida, Â.; Calisto, V.; Esteves, V.I.; Schneider, R.J.; Soares, A.M.V.M.; Figueira, E.; Freitas, R. Presence of the pharmaceutical drug carbamazepine in coastal systems: Effects on bivalves. *Aquat. Toxicol.* **2014**, *156*, 74–87. [CrossRef]

18. Tsiaka, P.; Tsarpali, V.; Ntaikou, I.; Kostopoulou, M.N.; Lyberatos, G.; Dailianis, S. Carbamazepine-mediated pro-oxidant effects on the unicellular marine algal species Dunaliella tertiolecta and the hemocytes of mussel Mytilus galloprovincialis. *Ecotoxicology* **2013**, *22*, 1208–1220. [CrossRef]

19. Rajendran, K.; Sen, S. Adsorptive removal of carbamazepine using biosynthesized hematite nanoparticles. *Environ. Nanotechnol. Monit. Manag.* **2018**, *9*, 122–127. [CrossRef]

20. Chtourou, M.; Mallek, M.; Dalmau, M.; Mamo, J.; Santos-Clotas, E.; Salah, A.B.; Walha, K.; Salvadó, V.; Monclús, H. Triclosan, carbamazepine and caffeine removal by activated sludge system focusing on membrane bioreactor. *Process Saf. Environ. Prot.* **2018**, *118*, 1–9. [CrossRef]

21. Wang, S.; Wang, J. Carbamazepine degradation by gamma irradiation coupled to biological treatment. *J. Hazard. Mater.* **2017**, *321*, 639–646. [CrossRef]

22. Tang, K.; Spiliotopoulou, A.; Chhetri, R.K.; Ooi, G.T.H.; Kaarsholm, K.M.S.; Sundmark, K.; Florian, B.; Kragelund, C.; Bester, K.; Andersen, H.R. Removal of pharmaceuticals, toxicity and natural fluorescence through the ozonation of biologically-treated hospital wastewater, with further polishing via a suspended biofilm. *Chem. Eng. J.* **2018**, *359*, 321–330. [CrossRef]

23. Hansen, K.M.S.; Spiliotopoulou, A.; Chhetri, R.K.; Escolà Casas, M.; Bester, K.; Andersen, H.R. Ozonation for source treatment of pharmaceuticals in hospital wastewater—Ozone lifetime and required ozone dose. *Chem. Eng. J.* **2016**, *290*, 507–514. [CrossRef]

24. Alharbi, S.K.; Price, W.E.; Kang, J.; Fujioka, T.; Long, D. Ozonation of carbamazepine, diclofenac, sulfamethoxazole and trimethoprim and formation of major oxidation products. *Desalin. Water Treat.* **2016**, *57*, 29340–29351. [CrossRef]

25. Dwivedi, K.; Rudrashetti, A.P.; Chakrabarti, T. Transformation Products of Carbamazepine (CBZ) After Ozonation and their Toxicity Evaluation Using *Pseudomonas* sp. Strain KSH-1 in Aqueous Matrices. *Indian J. Microbiol.* **2018**, *58*, 193–200. [CrossRef]

26. Hübner, U.; Seiwert, B.; Reemtsma, T.; Jekel, M. Ozonation products of carbamazepine and their removal from secondary effluents by soil aquifer treatment—Indications from column experiments. *Water Res.* **2014**, *49*, 34–43. [CrossRef]

27. Wang, B.; Zhang, H.; Wang, F.; Xiong, X.; Tian, K.; Sun, Y.; Yu, T. Application of heterogeneous catalytic ozonation for Refractory Organics in Wastewater. *Catalysts* **2019**, *9*, 241. [CrossRef]

28. Aghaeinejad-Meybodi, A.; Ebadi, A.; Shafiei, S.; Khataee, A.; Kiadehi, A.D. Degradation of Fluoxetine using catalytic ozonation in aqueous media in the presence of nano-γ-alumina catalyst: Experimental, modeling and optimization study. *Sep. Purif. Technol.* **2019**, *211*, 551–563. [CrossRef]

29. Chedeville, O.; Di Giusto, A.; Delpeux, S.; Cagnon, B. Oxidation of pharmaceutical compounds by ozonation and ozone/activated carbon coupling: A kinetic approach. *Desalin. Water Treat.* **2016**, *57*, 18956–18963. [CrossRef]

30. Ikhlaq, A.; Waheed, S.; Joya, K.S.; Kazmi, M. Catalytic ozonation of paracetamol on zeolite A: Non-radical mechanism. *Catal. Commun.* **2018**, *112*, 15–20. [CrossRef]

31. Saeid, S.; Tolvanen, P.; Kumar, N.; Eränen, K.; Peltonen, J.; Peurla, M.; Mikkola, J.P.; Franz, A.; Salmi, T. Advanced oxidation process for the removal of ibuprofen from aqueous solution: A non-catalytic and catalytic ozonation study in a semi-batch reactor. *Appl. Catal. B Environ.* **2018**, *230*, 77–90. [CrossRef]

32. Xu, Y.; Wang, Q.; Yoza, B.A.; Li, Q.X.; Kou, Y.; Tang, Y.; Ye, H.; Li, Y.; Chen, C. Catalytic ozonation of recalcitrant organic chemicals in water using vanadium oxides loaded ZSM-5 zeolites. *Front. Chem.* **2019**, *7*, 384. [CrossRef] [PubMed]

33. Aho, A.; Salmi, T.; Murzin, D.Y. Catalytic Pyrolysis of Lignocellulosic Biomass. *Role Catal. Sustain. Prod. Bio-Fuels Bio-Chem.* **2013**, 137–159. [CrossRef]

34. Somathilake, P.; Dominic, J.A.; Achari, G.; Cooper, H. Degradation of Carbamazepine by Photo-assisted Ozonation: Influence of Wavelength and Intensity of Radiation Degradation of Carbamazepine by Photo-assisted Ozonation: Influence of Wavelength and Intensity of Radiation. *Ozone Sci. Eng.* **2018**, *40*, 113–121. [CrossRef]

35. Cai, T.; Gao, Y.; Yan, J.; Wu, Y.; Di, J. Visual detection of glucose using triangular silver nanoplates and gold nanoparticles. *RSC Adv.* **2017**, *7*, 29122–29128. [CrossRef]

36. Han, Y.; Ma, M.; Li, N.; Hou, R.; Huang, C.; Oda, Y.; Wang, Z. Chlorination, chloramination and ozonation of carbamazepine enhance cytotoxicity and genotoxicity: Multi-endpoint evaluation and identification of its genotoxic transformation products. *J. Hazard. Mater.* **2018**, *342*, 679–688. [CrossRef] [PubMed]

37. Mcdowell, D.C.; Huber, M.M.; Wagner, M.; Von Gunten, U.; Ternes, T.A. Ozonation of carbamazepine in drinking water: Identification and kinetic study of major oxidation products. *Environ. Sci. Technol.* **2005**, *39*, 8014–8022. [CrossRef] [PubMed]

38. Gottschalk, C.; Libra, J.A.; Saupe, A. *Ozonation of Water and Waste Water*; Wiley-VCH: Weinheim, Germany, 2010; ISBN 9783527319626.

39. Einaga, H.; Maeda, N.; Nagai, Y. Comparison of catalytic properties of supported metal oxides for benzene oxidation using ozone. *Catal. Sci. Technol.* **2015**, *5*, 3147–3158. [CrossRef]

40. Rosal, R.; Rodríguez, A.; Gonzalo, M.S.; García-Calvo, E. Catalytic ozonation of naproxen and carbamazepine on titanium dioxide. *Appl. Catal. B Environ.* **2008**, *84*, 48–57. [CrossRef]

41. Kumar, N.; Mäki-Arvela, P.; Hajek, J.; Salmi, T.; Murzin, D.Y.; Heikkilä, T.; Laine, E.; Laukkanen, P.; Väyrynen, J. Physico-chemical and catalytic properties of Ru-MCM-41 mesoporous molecular sieve catalyst: Influence of Ru modification methods. *Microporous Mesoporous Mater.* **2004**, *69*, 173–179. [CrossRef]

42. Iodometric Method for the Determination of Ozone in a Process Gas. Available online: www.otsil.net/articles.html%0D (accessed on 2 January 2020).

43. Lin, W.C.; Chen, H.C.; Ding, W.H. Determination of pharmaceutical residues in waters by solid-phase extraction and large-volume on-line derivatization with gas chromatography-mass spectrometry. *J. Chromatogr. A* **2005**, *1065*, 279–285. [CrossRef]

44. Rossmann, J.; Schubert, S.; Gurke, R.; Oertel, R.; Kirch, W. Simultaneous determination of most prescribed antibiotics in multiple urban wastewater by SPE-LC-MS/MS. *J. Chromatogr. B Anal. Technol. Biomed. Life Sci.* **2014**, *969*, 162–170. [CrossRef] [PubMed]